KLYNE, W. & PRELOG, V. (1960). *Experientia*, **16**, 521–523.
LEUNG, Y. C. & MARSH, R. E. (1958). *Acta Cryst.* **11**, 17–31.
MAIN, P., WOOLFSON, M. M. & GERMAIN, G. (1971). *MULTAN. A Computer Program for the Automatic Solution of Crystal Structures.* Univ. of York Printing Unit, York, England.
PATTABHI, Y., VENKATESAN, K. & HALL, S. R. (1973). *Cryst. Struct. Commun.* **2**, 223–227.
RAMACHANDRAN, G. N. (1968). *Biopolymers*, **6**, 1494–1496.
RAMACHANDRAN, G. N. & KOLASKAR, A. S. (1973). *Biochim. Biophys. Acta*, **303**, 385–388.
STENKAMP, R. E. & JENSEN, L. H. (1973). *Acta Cryst.* B**29**, 2872–2878.
SUBRAMANIAN, E. (1967). *Acta Cryst.* **22**, 910–917.
THYAGARAJA RAO, S. (1969). *Z. Kristallogr.* **129**, 50–64.
UEKI, T., ASHIDA, T., KAKUDO, M., SASADA, Y. & KATSUBE, Y. (1969). *Acta Cryst.* B**25**, 1840–1849.
WINKLER, F. K. & DUNITZ, J. D. (1971). *J. Mol. Biol.* **59**, 169–182.

Acta Cryst. (1974). B**30**, 2613

A Neutron-Diffraction Study of Holmium Ethylsulfate Enneahydrate by the White-Radiation Method

BY CAMDEN R. HUBBARD,* CARL O. QUICKSALL† AND ROBERT A. JACOBSON

Ames Laboratory-USAEC and Department of Chemistry, Iowa State University, Ames, Iowa 50010, *U.S.A.*

(*Received* 1 *February* 1974; *accepted* 25 *June* 1974)

The structure of holmium ethylsulfate enneahydrate has been studied by the white-radiation neutron-diffraction method. Of 703 intensities collected in two days at the Ames Laboratory 5 MW reactor, 300 had $I > 3\sigma_I$. Linear programming proved to be an improved technique compared with least-squares procedures for unfolding the observed Laue intensities. The phased Fourier map, calculated using the unfolded structure factors, clearly revealed all hydrogen-atom positions, and the resulting peak heights were proportional to the neutron scattering lengths. A subsequent comparison of the Fourier and least-squares hydrogen atomic positions revealed that the average and maximum deviations were 0·17 and 0·28 Å. The structure was refined with isotropic thermal parameters to a final $RI_\omega = 0{\cdot}139$ and $RI_\omega^{\geq 3\sigma} = 0{\cdot}111$. Several improvements of the white-radiation method are suggested based on this study and previous results. The space group was confirmed to be $P6_3/m$. The holmium ion is at the center of a slightly distorted tricapped trigonal prism of water molecules. Each water oxygen is hydrogen bonded to two ethylsulfate ions. The hydrogen bonding and oxygen lone pair–lone pair interactions reduce the D_{3h} rare-earth ion site symmetry to C_{3h}. The orientation of the two types of water molecules relative to the holmium is somewhat different as are associated O–H distances (0·92 *vs.* 1·04 Å).

Introduction

Using two and three-dimensional X-ray diffraction techniques Fitzwater & Rundle (1959) investigated a number of hydrated rare-earth ethylsulfates, including the yttrium, erbium and praseodymium salts. These salts were all isomorphous, and in each the rare-earth ion was located at the center of a trigonal prism of water molecules, with additional water molecules capping each rectangular face. From a consideration of the oxygen–oxygen distances and appropriate angles, they hypothesized numerous hydrogen bonds; no hydrogen-atom positions were determined however.

Because of the continuing interest in the rare-earth metals and their compounds in the Ames Laboratory, and to accurately elucidate the hydrogen bonding in these salts and the interplay with the coordination forces, we decided to carry out a neutron investigation of a member of this series, $Ho(C_2H_5SO_4)_3.9H_2O$.

The second major goal of this research was to gain further experience with the recently developed white-radiation method (Hubbard, Quicksall & Jacobson, 1971; Hubbard, Quicksall & Jacobson, 1972, hereinafter HQJ). These previous studies indicated that structure determination was not only possible using the white-radiation method, but also yielded comparable precision to that of conventional monochromatic-beam techniques while permitting use of smaller crystals and rapid data collection.

Experimental

$Ho(C_2H_5SO_3)_3.9H_2O$, kindly supplied by Dr F. Spedding, was dissolved in distilled water and crystallized by slow evaporation. Initial studies indicated that a crystal of 9 mm^3 volume (maximum dimension 3 mm) was sufficient to give reasonable scattering. After being mounted on a thin vanadium rod, the hygroscopic crystal was encapsulated within a quartz

* Present address: Institute for Materials Research, National Bureau of Standards, Washington D. C. 20234, U.S.A.
† Present address: Department of Chemistry, Georgetown University, Washington D. C., U.S.A.

tube. The crystal was aligned with Mo $K\alpha$ X-rays. The resulting precession photographs indicated that the crystal was single and of good quality. The observed symmetry and systematic absences ($00l$, $l=2n+1$) were in agreement with Fitzwater & Rundle's space-group assignment $P6_3/m$. The hexagonal lattice constants were determined to be $a=13{\cdot}92$ (2) and $c=7{\cdot}03$ (1) Å. Based on the isomorphous Er and Y compounds, $Z=2$.

The neutron-diffraction data were collected at the 5 MW Ames Laboratory Research Reactor with an improved experimental arrangement over that described in HQJ. The neutron (and gamma) beam direct from the reactor core was filtered through a 1 mm thick foil of Eu–Al alloy (6·5% Eu). This foil preferentially attenuates the long wavelength portion of the incident flux (transmission factors of 0·95 at 1 Å and 0·42 at 3 Å). The beam was collimated by means of a convergent collimator resulting in a beam 5 mm in diameter with $\sim\frac{1}{8}°$ divergence at the collimator exit. The sample crystal was mounted on a conventional four-circle automated diffractometer centered 1 m from the reactor face. A boron nitride collimator with a 10 mm diameter acceptance hole was positioned directly in front of the BF_3 detector. Cadmium-lined tubes were employed as beam tunnels to bring the beam to within 7·5 cm of the crystal and to pass the diffracted beam to the detector. Together the beam tunnels and the boron nitride receiving collimator significantly reduced the number of air-scattered neutrons reaching the detector. The receiving collimator also improved the angular resolution such that background measurements with ω offsets of $\pm 1{\cdot}0°$ could be employed.

A source of high background at 2θ below 30° results from the main beam striking the counter shield. (The shield is a 20 cm diameter cylinder filled with borated paraffin containing an inner tube lined with cadmium surrounding the BF_3 detector.) A slot was milled into the side of this shield such that the main beam could pass unimpeded down to $2\theta=15°$. To obtain the minimum background above $2\theta=30°$ a polyethylene plug was inserted into the slot.

The crystal was centered on the diffractometer and the orientation determined from the known, lattice constants and three top/bottom–left/right centered reflections with 2θ fixed. The data-collection procedure followed that described in HQJ with $\hat{\lambda}=0{\cdot}65$, $n\hat{\lambda}$ initialized at 1·3 Å, and a counting period of 8×10^5 monitor counts (≈ 30 s). All Laue streaks with hkl positive and $d^*\leq 2\sin(40°)/1{\cdot}3$ (the maximum in φ_{eff} occurs near 1·3 Å) were measured in two groups: $2\theta\leq 30°$ with the counter shield plug removed and $2\theta>30°$ with the plug in place. Above $2\theta=80°$ no significant diffraction was observed. Three standard reflections were periodically measured. The maximum random intensity deviation in any standard was 3%. 703 intensities were recorded along 397 Laue streaks. With an ω offset of $\pm 1{\cdot}0°$ backgrounds were collected for all the data with $2\theta\leq 30$ and for about $\frac{1}{3}$ of the data above $2\theta=30°$. (The background is nearly independent of diffraction angle above $2\theta=30°$.) The data-collection period was just 2 days.

The observed backgrounds were plotted as a function of 2θ. A few spuriously high backgrounds were omitted (they are due to a tail of a strong Laue streak overlapping with a background measurement) and a smooth curve was obtained. I^{obs} and σ_I were obtained from equation (21) of HQJ with bg1 = bg2 as obtained from the background curve. A total of 300 intensities satisfied the condition $I^{\text{obs}}>3\sigma_I$. The quartz tube and, to a lesser extent, the vanadium rod contribute to the background scattering and reduce the ratio of diffracted intensity to background.

The linear attenuation coefficient was approximated using the values for hydrogen incoherent scattering (see HQJ) and true absorption (Bacon, 1962) as $\mu(\lambda)=2{\cdot}2+2{\cdot}1*[(\lambda/1{\cdot}08)-1]\ \text{cm}^{-1}$. This expression for $\mu(\lambda)$ is adequate for the approximate wavelength range $0{\cdot}7\leq\lambda\leq 3{\cdot}0$ Å. The calculated transmission factors $T(\mu_0)$ ranged from 0·68 to 0·75 [$\mu_0=\mu(1{\cdot}08\ \text{Å})=2{\cdot}2$]. The derivatives $\partial T/\partial\mu|_{\mu_0}$ and $\partial^2 T/\partial^2\mu|_{\mu_0}$ were approximately $\frac{1}{7}$ and $\frac{1}{35}$ of $T(\mu_0)$, respectively. Although the Taylor series expansion [equation (11) of HQJ] for $T(\mu)$ exhibits greater error for larger λ's, the effective flux, attenuation, and extinction all significantly reduce the importance of long wavelengths in the intensity sum. The inability to accurately calculate μ_0 and μ' is a source of systematic error in structure refinement. Possible approaches to eliminate this problem will be discussed later.

Calculations with the NaCl data from HQJ indicate that the maximum error in calculated intensity due to an artificial limit $\lambda_{\text{max}}=3{\cdot}3$ Å is less than 1% of I^{calc}. Based on this result and the known small importance of long wavelengths, the finite range of λ used in least-squares refinement and calculation of structure factors was from 0·5 to 3·3 Å.

Obtaining the model

The intensity at any θ along the Laue 'streak' is given by [(5) of HQJ]

$$I_h^{\text{obs}}(\theta)=K\sum_n \varphi_{\text{eff}}(\lambda_n)T(\lambda_n)y(\lambda_n)\,[F_{nh}/d^*_{nh}]^2 \qquad (1)$$

where K is the scale factor, $\lambda_n=2d_{nh}\sin(\theta)$, φ_{eff} is the effective flux, T is a transmission factor, y is an extinction correction and F_{nh} is the structure factor. Previously the structure factors were determined from the observed intensities by a least-squares technique. This approach had several undesirable features. Along dense lattice rows the calculated squared structure factors, $|F_{nh}|^2$, tended to oscillate for larger values of n, and negative $|F_{nh}|^2$ can result.

A technique based on linear programming (Kreko, 1968) has been used to eliminate the instabilities of the least-squares technique.

The system of equations to be solved [equation (5) of HQJ] is,

$$\mathbf{G} \cdot F^2 = I^{\text{obs}} \tag{2}$$

where the vector of m observations along one streak is I^{obs}, the matrix $\mathbf{G}$ includes flux, transmission and geometric factors, and F^2 is the vector of n unknowns ($n \leq m$). Since the maxima of $\varphi_{\text{eff}}(\lambda)$ occurs near $\lambda =$ 1·3 Å, n can be limited to $2 \sin(\theta_{\max})/(1{\cdot}3d^*_{hh})$. The system of equations is non-linear in $|F|^2$ if extinction is included in equation (2), but extinction effects are usually small and can be included by a cyclic method if an estimation of the extinction parameters can be made prior to the solution of the structure.

Ideally, the solution to equation (2) will produce $|F|^2$ greater than zero and less than some maximum which is dependent on the structure. Linear programming can incorporate these limits in a straightforward manner thereby eliminating the nonphysical negative values and the diverging oscillations about zero. We chose to weight the individual observations and to minimize the maximum error between the observed and calculated intensities. To achieve this, equation (2) must be rewritten as a pair of inequalities

$$\begin{aligned} \mathbf{G} \cdot F^2 - \varepsilon\sigma &\leq I^{\text{obs}} \\ \mathbf{G} \cdot F^2 + \varepsilon\sigma &\geq I^{\text{obs}}. \end{aligned} \tag{3}$$

Slack variables were added for solution by the modified simplex method (Kreko, 1968). To use this technique the set of observed intensities was modified by setting the few $I^{\text{obs}} < 0$ equal to 0; no extinction correction was included. Approximately 40% of the lattice rows involved more data than structure factors to be calculated ($n < m$). For these rows the maximum error ε was typically 0·25 standard deviations. The largest two ε's obtained were 2·50 and 1·41 standard deviations. No oscillation of high-order structure factors was observed.

The unfolded $|F|$'s were phased on the rare earth, oxygen, sulfur, and carbon parameters ($\approx \frac{1}{2}$ the atoms in the unit cell); the scale factor was refined. The conventional R value obtained was 0·50. The phased structure factors were then used to calculate a Fourier map. In addition to clearly revealing the missing hydrogen-atom positions, the map also exhibited peak heights in good agreement with the scattering power of each atom as shown in Table 1. No deviations from the space group $P6_3/m$ were indicated in this map confirming Fitzwater & Rundle's choice. The ethyl hydrogens were significantly more diffuse than were the water hydrogens. The independent $-CH_2-$ hydrogen was quite elongated along the z axis. These observations qualitatively agree with the thermal parameters obtained from the least-squares refinement to be discussed below. The subsequent comparison of the initial and final hydrogen atomic positions revealed that the average and maximum errors were 0·17 and 0·28 Å (Fourier grid resolution was 0·43 × 0·43 × 0·22 Å). Although this exceptional agreement may be partially fortuitous, linear programming did provide an excellent set of structure factors.

Table 1. *Observed peak heights and scattering factors for all atoms*

	Ho	C	O	S	H
$b(\times 10^{-13}$ cm)	8·5	6·61	5·77	3·1	−3·78
Peak height	30	16 to 18	16 to 20	10	−7 to −8

Refinement

The least-squares refinement was completed with *WIRALS*, a full-matrix least-squares program, which minimizes $\sum w_i(I_i^{\text{obs}} - I_i^{\text{calc}})^2$. *WIRALS* corrects the calculated data for extinction and absorption before comparing the calculated and observed intensities. For this work the weighted R value is defined as

$$RI_w = \{w_i(I_i^{\text{obs}} - I_i^{\text{calc}})^2 / \sum w_i(I_i^{\text{obs}})^2\}^{1/2}$$

where $w_i = 1/\sigma_i^2$. Since the sum contains a large fraction of data with $I_i^{\text{obs}} < 3\sigma_I$, RI_w will also be reported for that data with $I > 3\sigma$, termed $RI_w^{>3\sigma}$. All observations, including a few with $I^{\text{obs}} < 0$, were used in the least-squares refinement.

The initial model consisted of the rare-earth, oxygen, carbon, sulfur parameters (Fitzwater & Rundle, 1959) and the hydrogen positions from the phased Fourier map for the space group $P6_3/m$. Isotropic thermal parameters for the water and ethyl hydrogens were set at 2 and 3 Å^2, respectively. The flux parameters (see HQJ) were estimated to be $P1 = 2{\cdot}56$ and $P2 = 0{\cdot}3$, with $P3$ fixed at 3·0. A type I extinction correction was assumed with $g = 1000$ (Zachariasen, 1967). The scattering lengths used were $b_{\text{Ho}} = 8{\cdot}5\text{f}$,* $b_{\text{O}} = 5{\cdot}77\text{f}$, $b_{\text{C}} = 6{\cdot}61\text{f}$, $b_{\text{S}} = 3{\cdot}1\text{f}$ and $b_{\text{H}} = -3{\cdot}78\text{f}$ (*International Tables for X-ray Crystallography*, 1962). After initial refinement of the scale factor and positional parameters, $RI_w = 0{\cdot}25$. Throughout the next seven cycles of refinement the calculated shifts were damped because of the significant correlation ($\approx 0{\cdot}9$) between K, $P1$ and $P2$ and moderate correlation (up to 0·3) of g with several B's. These seven cycles of refinement of K, $P1$, $P2$, g and all positional parameters lowered RI_w to 0·174. Isotropic thermal parameters were then included in the list of variables. Three more cycles of damped refinement followed by three cycles of undamped refinement decreased RI_w to 0·139 ($RI_w^{>3\sigma} = 0{\cdot}111$). On the final cycle all shifts were less than 0·02 times the corresponding estimated error. The standard deviation of an observation of unit weight was 0·98. Both type II and general extinction (Zachariasen, 1967) were tested. The least-squares analysis indicated that the data were insensitive to the domain radius. The crystal was then assumed to exhibit type I extinction. Anisotropic thermal motion refinement was also attempted. Although both R values dropped about 0·02 two resultant

* $\text{f} = 10^{-13}$ cm.

Table 2. *Observed and calculated Laue intensities*

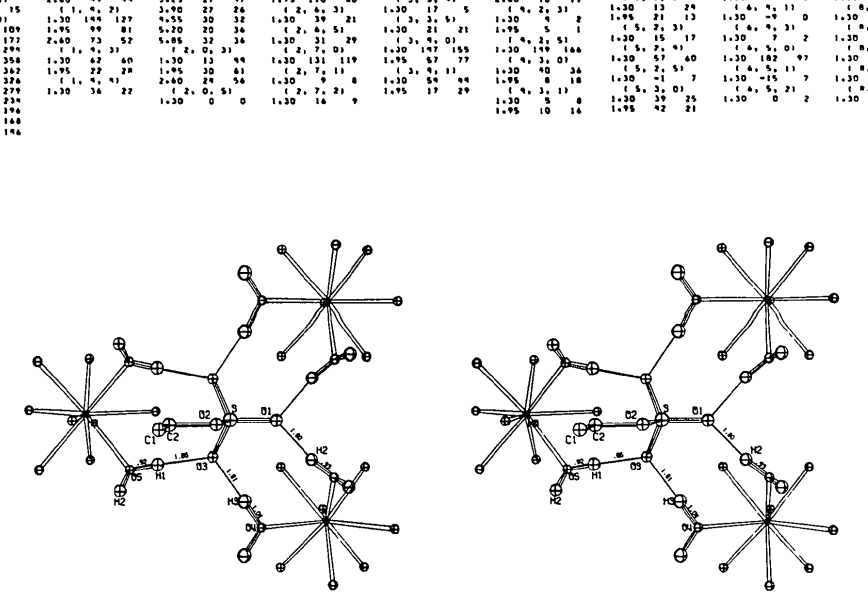

Fig. 1. Stereo diagram of the ethylsulfate environment viewed approximately down the [110] axis. Hydrogen bonds shown as light lines.

thermal ellipsoids were non-positive definite. It was concluded that the absorption correction was probably not adequate for anisotropic refinement and that the isotropic results are the best attainable model. However, the indication of the anisotropic refinement and Fourier map was that there exists significant thermal motion along the c axis for the ethylsulfate carbon and hydrogen atoms. Ignoring this thermal motion, of course, will affect the calculated bond lengths of these atoms as well as influence the isotropic thermal parameters. The observed and calculated Laue intensities are listed in Table 2.

The final atomic parameters and estimated standard deviations are listed in Table 3. The e.s.d.'s were obtained from the inverse matrix of the least-squares analysis. The final scale, flux and extinction parameters were $K=102$ (12), $P1=2{\cdot}79$ (0·08), $P2=0{\cdot}34$ (0·05) and $g=14700$ (1300). The e.s.d.'s of K, $P1$ and $P2$ are approximately double those obtained from NaCl in HQJ; the e.s.d. for g is nearly 50% greater than in α-oxalic acid. The decreased precision could be due to the choice of $\hat{\lambda}=0{\cdot}65$; in the initial test of the method on α-oxalic acid, a $\hat{\lambda}$ of 0·325 Å was used. The latter value would have yielded more independent data along each Laue 'streak' and could possibly have enabled meaningful refinement of anisotropic thermal parameters.

Table 3. *Atomic parameters and their estimated standard deviations*

x, y and z are fractional coordinates $\times 10^4$. The e.s.d.'s $\times 10^4$ are enclosed in parentheses. B is the isotropic temperature factor with e.s.d.'s $\times 10^2$ in parentheses.

	x	y	z	B
Ho	6667	3333	2500	0·55 (28)
S	3177 (26)	−0535 (25)	2500	3·42 (74)
O(1)	2460 (13)	−1735 (14)	2500	2·56 (32)
O(2)	2284 (14)	−0130 (13)	2500	2·61 (33)
O(3)	3844 (08)	−0100 (07)	0779 (14)	2·10 (21)
O(4)	4964 (13)	3522 (11)	2500	1·49 (27)
O(5)	5453 (08)	2120 (08)	0094 (09)	1·57 (18)
H(1)	4990 (14)	1367 (15)	0345 (26)	2·99 (38)
H(2)	5074 (14)	2353 (13)	−0711 (28)	2·61 (33)
H(3)	4633 (13)	3674 (15)	1278 (29)	3·60 (43)
H(4)	3286 (21)	1429 (22)	1284 (45)	9·04 (81)
H(5)	2131 (28)	2174 (31)	2500	5·51 (83)
H(6)	1350 (26)	1012 (27)	1303 (41)	11·3 (110)
C(1)	1825 (13)	1284 (14)	2500	2·88 (35)
C(2)	2723 (14)	1043 (14)	2500	3·11 (31)

Discussion of the structure

The major difference between the erbium, yttrium praseodymium and holmium ethylsulfate structures is solely due to the changing ionic radius of the rare-earth ion. The hydrogen bonding of the holmium structure should be typical for all four rare-earth ethylsulfates. Figs. 1 and 2, both viewed approximately down the [110] axis, show the important features of the hydrogen bonding. The ethyl hydrogens have been omitted for clarity in both drawings. Fig. 1 emphasizes the environment about an ethylsulfate ion. Fig. 2 depicts the holmium enneahydrate moiety surrounded by the nine nearest neighbor ethylsulfate groups. The ethylsulfate ($z=\frac{1}{4}$) behind the holmium enneahydrate has been omitted in this figure.

The holmium ion is nine-coordinate, with three water oxygens above the mirror plane and three below forming the vertices of a trigonal prism. Three additional water oxygens lie in the mirror plane and approximately cap the rectangular faces of the trigonal prism. The ethylsulfate ions lie primarily in the mirror plane with an O–S–O–C–C–H chain in this plane. Table 4 lists the important bond distances and angles. The standard deviations were calculated with *ORFFE* (Busing, Martin & Levy, 1964).

As predicted, the C_{3h} symmetry about the rare-earth ion, instead of D_{3h}, is a result of the hydrogen bonding. The two hydrogen bonds from the trigonal prism water oxygens are of unequal length, 1·86 (2) and 1·80 (2) Å.

The hydrogen bonding is typical with H···O distances ~1·8 Å and O–H···O angles of ~170° and is essentially that predicted by Fitzwater & Rundle (1959). Both the H(1)–O(5)–H(2) angle of 108·2 (1·5)° and H(3)–O(4)–H(3)^m angle of 111·2 (2·1)° indicate essentially sp^3 hybridization for the water oxygens. The O(4) lone-pair orbitals are in the mirror plane and are necessarily equally involved in their interaction with the rare-earth ion. Thus the electric dipole is directed

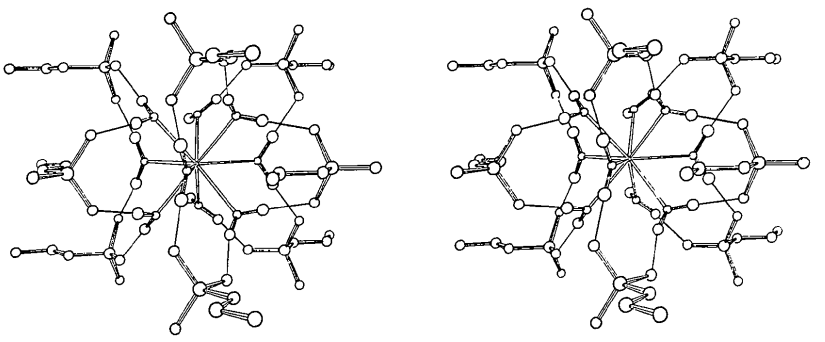

Fig. 2. Stereo diagram of the holmium enneahydrate moiety surrounded by nearest neighbor ethylsulfate ions viewed approximately down the [110] axis. The ethyl hydrogens have been omitted as well as the ethylsulfate directly behind the $Ho(H_2O)_9$ moiety.

Table 4. *Selected bond distances* (Å) *and angles* (°)

Holmium enneahydrate

Ho—O(4)	2·474 (15)	H(1)–O(5)–H(2)	108·2 (1·5)
Ho—O(5)	2·373 (11)	H(3)–O(4)–H(3)^m	111·2 (2·1)
O(5)–O(5)^i	2·884 (17)	Ho—O(5)–H(2)	120·8 (1·2)
O(5)–O(5)^m	3·382 (24)	Ho—O(4)–H(3)	123·4 (1·0)
O(5)–O(4)	2·880 (16)	Ho—O(5)–H(1)	120·0 (1·4)
O(5)^i–O(4)	2·648 (16)		
O(4)–O(4)^i	4·287 (27)		
O(5)–H(1)	0·920 (25)		
O(5)–H(2)	0·926 (27)		
O(4)–H(3)	1·041 (24)		

Ethylsulfate

S—O(1)	1·435 (31)	O(1)–S—O(3)	113·7 (1·4)
S—O(3)	1·453 (18)	O(3)–S—O(3)^m	112·7 (2·2)
S—O(2)	1·578 (33)	O(3)–S—O(2)	107·2 (1·4)
O(2)–C(2)	1·409 (21)	S—O(2)–C(2)	116·0 (1·8)
C(2)–C(1)	1·425 (19)	O(2)–C(2)–H(4)	110·3 (1·6)
C(2)–H(4)	1·095 (36)	O(2)–C(2)–C(1)	109·9 (1·5)
C(1)–H(5)	1·075 (45)	C(2)–C(1)–H(5)	111·9 (2·1)
C(1)–H(6)	1·015 (34)	C(2)–C(1)–H(6)	112·7 (1·7)
		H(6)–C(1)–H(6)^m	112·1 (3·2)
		H(5)–C(1)–H(6)	103·3 (1·9)

Hydrogen-bond distances and angles

H(1)···O(3)	1·857 (19)	O(5)—H(1)···O(3)	169·7 (1·6)
H(2)···O(1)	1·799 (24)	S—O(3)···H(1)	126·9 (1·4)
H(3)···O(3)	1·805 (22)	O(5)—H(2)···O(1)	165·9 (1·6)
		S—O(1)···H(2)	127·9 (1·0)
		O(4)—H(3)···O(3)	175·2 (1·5)
		S—O(3)···H(3)	123·3 (1·4)
		H(3)—O(3)···H(1)	109·8 (1·0)

Symmetry operations

i $(xyz) \rightarrow (1{\cdot}0+y-x, 1{\cdot}0-x, z)$
m $(xyz) \rightarrow (x, y, \frac{1}{2}-z)$

at the rare-earth ion. However, only one sp^3 lone pair from O(5) is directed toward the rare-earth ion. The other lone-pair orbital is nearly tangential to the base of the trigonal prism and is directed toward an adjacent H(2). Hence, the O(5) water dipole is directed into the interior of the trigonal prism but not directed at the rare-earth ion.

A comparison of rare earth–oxygen and ethylsulfate bond distances for Ho, Er, Y and Pr is given in Table 5. The non-hydrogen bond distances of the ethylsulfate group agree within 2σ with Fitzwater & Rundle's (1959) X-ray structures except for the C–C distance [1·43 (2) Å compared to 1·49 Å]. The calculated ethylsulfate bond angles are all in agreement with expected tetrahedral angles. The holmium–oxygen distances exhibit the same trends as were found in the Er, Y and Pr structures: a longer distance to the capping oxygen ($z=\frac{1}{4}$) than to the trigonal prism oxygens. The rare earth–trigonal prism oxygen distance ($2{\cdot}373 \pm 0{\cdot}011$ Å) in this structure is essentially identical with that found in both the Er and Y structures (Fitzwater & Rundle, 1959). (In the Pr structure only two-dimensional data were collected.) However, the rare earth–capping oxygen distance ($2{\cdot}474 \pm 0{\cdot}015$ Å) has decreased from the Er distance of 2·52, the Y distance of 2·55 and Pr distance of 2·65 Å. Since the structures are essentially isomorphous, this trend can be ascribed to an ionic radius effect. The ionic radii for the trivalent ions Ho, Er, Y and Pr are 0·894, 0·950, 0·98 and 1·013 Å respectively (Cotton & Wilkinson, 1962). The trigonal prism oxygen–rare earth distance, which remained fixed, is probably controlled by electron lone-pair–lone-pair repulsions while the capping oxygen–rare-earth distance is not.

Table 5. *Comparison of selected distances of* $RE(C_2H_5SO_4)_3.9H_2O$

	Ho*	Er†	Y†	Pr†
RE—O(4)	2·474 (15) Å	2·52 Å	2·55 Å	2·65 Å
RE—O(5)	2·373 (11)	2·37	2·37	(2·47)
S—O(1)	1·435 (31)	1·45	1·45	1·46
S—O(3)	1·453 (18)	1·44	1·46	(1·45)
S—O(2)	1·578 (33)	1·60	1·57	1·60
O(2)–C(2)	1·409 (21)	1·44	1·52	1·40
C(1)–C(2)	1·425 (19)	1·50	1·47	1·54

* This work.
† Fitzwater & Rundle (1959).

The water molecule O–H distances appear to be affected by the metal–oxygen interaction. The trigonal prism water O–H distances, 0·920 (25) and 0·926 (27) Å, are shorter than the capping water O–H distance, 1·041 (24) Å. The unusually short trigonal prism water O–H distances are consistent with a shift in hybridization of the oxygen giving greater *p*-character to the lone-pair orbitals and consequently greater *s*-character to the O–H bonds.

Discussion of the white-radiation method

Several improvements in the experimental equipment were incorporated in this study. The linear programming technique for unfolding the Laue intensities proved exceptionally effective. The resultant Fourier map using the derived structure factors clearly indicated all hydrogen-atom positions. Even the peak profiles were in good qualitative agreement with the thermal parameters obtained by least-squares refinement. We feel that linear programming has essentially solved the unfolding problem.

The question of structural accuracy is of concern. Today, the monochromatic-beam technique certainly provides the most accurate structural model (Wilson & Cooper, 1973). Undoubtedly this is because of inadequacies in the techniques used for absorption and extinction corrections in the white-radiation method as well as the necessity of mathematically representing the flux distribution. The precision of a crystal structure determination can be partially judged by the estimated errors in bond distances and angles. With the monochromatic-beam technique one expects $\sigma(\text{bond}) \leq 0{\cdot}005$ Å and $\sigma(\text{angle}) \leq 0{\cdot}5°$. For the white-radiation technique the average standard deviations for $Ho(C_2H_5SO_4)_3.9H_2O$ are $\sigma(\text{bond}) = 0{\cdot}02$ Å and $\sigma(\text{angle}) = 1{\cdot}5°$ and for α-oxalic acid dihydrate are $\sigma(\text{bond}) = 0{\cdot}008$ Å and $\sigma(\text{angle}) = 0{\cdot}9°$. The lower accuracy in the Ho study can be attributed to

several factors; (1) use of $\hat{\lambda}=0{\cdot}65$ compared to 0·325; (2) the necessity of using a quartz capillary; (3) the poor quality of the Ho crystal compared with the α-POX crystal; and (4) the greater difficulty in correcting for attenuation. Three important questions about the white-radiation method should still be considered. First, how can the inadequacies be minimized? Second, how serious are these inadequacies? Finally, what do we gain by using the white-radiation method?

To improve the model for the flux distribution, intensity data along one or more lattice rows could be collected using a small $\hat{\lambda}$, say 0·05 Å. This data could be used to refine the flux parameters independent of the refinement of the structural model. Comparison of the α-POX and Ho results indicates that a choice of $\hat{\lambda}$ closer to 0·325 Å instead of 0·65 Å improves the structural model. Obviously choosing a large $\hat{\lambda}$ will result in a small data set while choosing a small $\hat{\lambda}$ will result in a large data set. The larger data set should yield a better structural model. One can conceivably select a $\hat{\lambda}$ based on the questions to be answered in the study. For example, are anisotropic thermal parameters required or is a skeletal model adequate?

The excellent agreement between anisotropic thermal parameters in α-POX by the white-radiation and monochromatic techniques is reassuring. The method is capable of acceptable results. The low precision in the Ho structure reported here is annoying but does not prevent the interpretation of the hydrogen-bonding scheme and its effect on the $Ho(H_2O)_9$ packing. The difficulties probably resulted from poor attenuation corrections. Several possibilities do exist for improving this situation in the future. The simplest solution is to deuterate the material. Alternatively the wavelength dependence of μ can be determined experimentally for the particular sample. A third possibility is to include μ_0' as a variable in the least-squares program. Also, the choice of λ_0 (taken equal to 1·08 Å for convenience of using existing tables to calculate μ_0 and μ_0') could be optimized to improve the accuracy of the Taylor series approximation [equation (11) of HQJ].

The advantages of the white-radiation technique are the use of smaller crystals and higher data rates. Instead of attempting a few problems a year we can now consider a few problems a month. In addition, this technique could readily be used at smaller reactors where the monochromatic technique would fail because of lack of flux.

The authors would like to acknowledge the assistance of Dr Vince Sposito of the Iowa State University Statistics Department for his assistance with the linear programming. One author (CRH) gratefully acknowledges the use of the National Bureau of Standards facilities for the final stages of refinement and preparation of this manuscript.

References

BACON, G. E. (1962). *Neutron Diffraction.* Oxford Univ. Press.

BUSING, W. R., MARTIN, K. O. & LEVY, H. A. (1964). *ORFFE.* Report ORNL-TM-306, Oak Ridge National Laboratory, Oak Ridge, Tennessee.

COTTON, F. A. & WILKINSON, (1962). *Advanced Inorganic Chemistry*, p. 877. New York: John Wiley.

FITZWATER, D. R. & RUNDLE, R. E. (1959). *Z. Kristallogr.* **112**, 362–374.

HUBBARD, C. R., QUICKSALL, C. O. & JACOBSON, R. A. (1972). *Acta Cryst.* A**28**, 236–245.

HUBBARD, C. R., QUICKSALL, C. O. & JACOBSON, R. A. (1971). *Nucl. Instrum. Methods*, **94**, 185-186.

International Tables for X-ray Crystallography (1962). Vol. III. Birmingham: Kynoch Press.

KREKO, B. (1968). *Linear Programming*, translated from the German by J. H. L. AHRENS & C. M. SAFE. Pitman: London.

WILSON, S. A. & COOPER, M. J. (1973). *Acta Cryst.* A**29**, 90–91.

ZACHARIASEN, W. H. (1967). *Acta Cryst.* **23**, 558–564.